Recombinant soluble IFN receptor (sIFNAR2) exhibits intrinsic therapeutic efficacy in a murine model of Multiple Sclerosis

M. Suardíaz [a, d, *], D. Clemente [b, d], C. Marin-Bañasco [a], T. Orpez [a], I. Hurtado-Guerrero [a], J. Pavía [c], M.J. Pinto-Medel [a, d], F. De Castro [b, d], L. Leyva [a, d], O. Fernández [a, d], B. Oliver [a, d]

[a] Unidad de Gestión Clínica Inter-centros de Neurociencias, Laboratorio de Investigación y Servicio de Neurología, Instituto de Biomedicina de Málaga (IBIMA), Hospitales Universitarios Regional de Málaga y Virgen de la Victoria, 29009, Málaga, Spain
[b] Grupo de Neurobiología del Desarrollo-GNDe, Hospital Nacional de Parapléjicos, 45071, Toledo, Spain
[c] Departamento de Farmacología, Facultad de Medicina, Universidad de Málaga, Instituto de Biomedicina de Málaga (IBIMA), 29009, Málaga, Spain
[d] Red Española de Esclerosis Múltiple (REEM), Spain

a b s t r a c t

Endogenous interferon beta (IFNβ) is an important cytokine involved in several chronic inflammatory diseases, such as Multiple Sclerosis (MS). In spite of the numerous therapeutic approaches available for MS patients, the administration of recombinant IFNβ continues being one of the first line treatment to these patients. The soluble form of IFNβ receptor (sIFNAR2) could act as critical regulator of the endogenous and the systemically administered IFNβ, but whether it functions as an agonist or antagonist of its ligand is not completely elucidated. Morover, the possible role of sIFNAR2 in autoimmune diseases like MS is still unknown and so far overlooked. Here we evaluated the efficacy of the combined therapy of IFNβ and our recombinant protein analogous to human sIFNAR2 as a treatment in a chronic mice model of MS (CP-EAE). We also tested the effect of the sIFNAR2 administered as a monotherapy over these EAE-animals. The results showed that our recombinant sIFNAR2 protein potentiates the immunomodulatory effects of exogenous IFNβ in CP-EAE by increasing the reduction of the induced inflammation and the tissue damage. Furthermore, we demonstrate for the first time that sIFNAR2 shows intrinsic properties by modulating the CP-EAE progression and the neuroinflammation processes related to this disease. Another intrinsic activity showed by sIFNAR2 is the inhibition of the T cells proliferation, which increase its potential as therapeutic molecule.

1. Introduction

Multiple Sclerosis (MS) is a chronic autoimmune disorder characterized by inflammation of the central nervous system (CNS). Endogenous interferon beta (IFNβ) is one of the cytokines involved in the pathology of MS, contributing for the maintenance of the anti-inflammatory status (Severa et al., 2015). Moreover, recombinant IFNβ continues being one of the most widely prescribed drug for MS patients, in spite of the numerous treatments available nowadays (Garg and Smith, 2015).

IFNβ mediates a variety of biologic responses, including antiviral, antiproliferative, and immunomodulatory effects. Its action is exerted through interaction with the interferon α/β cell surface receptor (IFNAR), composed of two subunits, i.e. IFNAR1 and IFNAR2, followed by activation of the intracellular Jak/STAT pathway that concludes with the activation of the genes containing the interferon stimulated response element (ISRE) and the induction of proteins, among others, the myxovirus-resistance protein A (MxA) with antiviral activity (Platanias, 2005).

Several soluble forms of many cytokine receptors have been proposed as critical cytokine regulators by providing mechanisms for modulating their responses (Fernandez-Botran, 1991, 1999, 2000). These receptors are able to bind to their ligand and can act as antagonists by competing with the cell surface receptor for cytokine binding. Otherwise, they can function as agonists serving as carrier proteins to protect the ligand from proteolysis and improving its stability (Fernandez-Botran, 2000; Rose-John and Heinrich, 1994). Therefore, these soluble receptors have been used

as promising therapeutic targets for the treatment of chronic inflammatory diseases (Fischer et al., 2015; Probert, 2015).

There are two major mechanisms for the generation of soluble receptors, alternative splicing of the RNA that encodes the cytokine receptor and cleavage of the membrane receptor(Fernandez-Botran, 2000). In this context, an alternative splicing of IFNAR2 gene generates three isoforms: the short form, that is a non-functional transmembrane protein, the long form which composes the functional receptor together with IFNAR1, and the soluble form (sIFNAR2), which lacks the transmembrane and cytoplasmic domains (Domanski et al., 1995; Novick et al., 1995), and can be detected in body fluids (Novick et al., 1992). It has been demonstrated that sIFNAR2, depending on concentration, lead to neutralization or augmentation of IFNb bioactivity(McKenna et al., 2004), being proposed as an important regulator of not only the endogenous but also the systemically administered type I IFNs (Hardy et al., 2001). Moreover, a recent study shows that sIFNAR2 over-expressing transgenic mice are more susceptible to TLR4-mediated septic shock than wild type mice, by directly exacerbating type I IFN signalling. They demonstrated that sIFNAR2 is an important agonist of endogenous IFN activity and also is likely that modulates the efficacy of clinically administered IFNs (Samarajiwa et al., 2014).

In spite of these evidences, the mechanism of action of sIFNAR2 in autoimmune diseases like MS is still unknown and so far overlooked.

Given all theses antecedents, we cloned, expressed, and purified a human recombinant sIFNAR2 protein in order to investigate whether sIFNAR2 may potentiate the efficacy of administered IFNb for clinical purpose, and also, to evaluate its potential intrinsic properties. To do so, sIFNAR2 has been administered combined with IFNb and also as a monotherapy in an experimental model of MS (chronic-progressive Experimental Autoimmune Encephalomyelitis, CP-EAE), which is the most frequently used T-cell-mediated CNS demyelination model for MS research (Denic et al., 2011; Friese et al., 2006; Moline ,-Vela ,zquez et al., 2015; Moreno et al., 2012; Steinman and Zamvil, 2005, 2006).

2. Material and methods

2.1. Cloning of human sIFNAR2

The protocol for the cloning, expression and purification of recombinant sIFNAR2 has been previously published (Orpez-Zafra et al., 2015). Briefly, the prokaryotic expression system pEcoli-Cterm 6xHN Linear (Clontech®) was chosen to ligate the sIFNAR2 insert. DH5a Competent Cells™ (Invitrogen®) were transformed with the plasmid and the colony forming units were isolated. After plasmid purification (PureYield™ (Promega®)) and once the nucleotide sequence and the correct reading frame were verified, BL21(DE3) (Invitrogen®) bacteria were transformed to produce the recombinant sIFNAR2. This was purified on high-capacity Ni^{2+}-iminodiacetic acid resin columns, detected by Western Blot using anti-IFNAR2 Human MaxPab (Abnova®) and confirmed its identity by matrix-assisted laser desorption/ionization time of flight (MALDI-TOF) mass spectrometry (Fig. 1). As a result, we have a human recombinant sIFNAR2 protein with 249 aminoacids and a molecular weight of 29 kDa, including the $(NH)_6$ tag.

2.2. Purification of the recombinant sIFNAR2 protein for mouse administration

Soluble 6xHN-tagged sIFNAR2 protein from *E. coli* BL21(DE3) cell extracts was purified by immobilized-metal affinity chromatography (IMAC) using a 1 ml HiTrapTM FF crude column (GE Healthcare) on an ÅKTA FPLC system (GE Healthcare) according to standard procedures. Fractions were analyzed in 10% SDS-polyacrylamide gels stained with Coomassie Brilliant Blue (BIO-RAD). 20 mM sodium phosphate, 0.5 M NaCl, 40 mM imidazole, pH 8.0 was used as binding buffer and 20 mM sodium phosphate, 0.5 M NaCl, 0.5 M imidazole, pH 7.4 was the elution buffer. The sIFNAR2 recombinant protein from different fractions was pooled, dialyzed against PBS and then quantified and loaded on a gel. Then, the final product with a purity higher 95% was stored at −80 °C until use. Protein densitometry was performed using the software ImageJ 1.440 (HIH, Bethesda, MD) to determine the concentration of sIFNAR2.

2.3. Endotoxin assay

The endotoxin level was determined using the Endosafe®-PTS™ system and the "Limulus Amebocyte Lysate (LAL) Test Cartridges with a sensitivity of 0.005 EU/ml" (Charles River Laboratories). Endotoxin of the purified sIFNAR2 was less than 1 EU/mg, which was considered to be acceptable for animal use (Malyala and Singh, 2008).

2.4. Mice

All experiments were conducted using adult (6e8 weeks old) female C57BL/6 (H2b) mouse inbred strain, purchased from Charles Rivers (Germany). The animals were housed in clear plastic cages under specific pathogen-free conditions in accordance with institutional guidelines. A controlled temperature (23 ± 1 °C), a 12:12-h light/dark cycle and free access to food and water were set. The study was approved by the Ethics and Research Committee of the University Regional Hospital of Ma ,laga, and all experiments were performed in compliance with the European Animal Research Laws (European Communities Council Directives 2010/63/EU, 90/219/EEC, Regulation (EC) No. 1946/2003) and the Spanish National and Regional Guidelines for Animal Experimentation and Use of Genetically Modified Organisms (Real Decreto 53/2013 and 178/2004, Ley 32/2007 and 9/2003, Decreto 320/2010).

2.5. EAE induction and clinical evaluation

CP-EAE was induced in mice by subcutaneous (s.c) immunization in the flanks with 200 mg of the Myelin Oligodendrocyte Glycoprotein peptide (MOG_{33e35}; MEVGWYRSPFSRVVHLYRNGK) (GenScript), emulsified in complete Freund's adjuvant containing 0.8 mg/ml of heat-inactivated *Mycobacterium tuberculosis* (Becton Dickinson), at a final volume of 100 ml. Pertussis toxin was administered intraperitoneally (i.p) at the dose of 300 ng (Sigma-Aldrich Química, S.L), injected the day of immunization and two days later.

The clinical score was blindly registered according to a standard 0 to 5 scale (Marin-Ba asco et al., 2014; Moline ,-Vela ,zquez et al., 2011, 2014): 0, healthy; 0.5, flaccidity and partial paralysis of the tail; 1, limp tail; 1.5, weakness in one hind limb; 2, hind limb paresis; 2.5, partial hind limb paralysis; 3, total hind limb paralysis; 3.5, partial fore limb paralysis; 4, hind limb paralysis; 4.5, body/front limb paresis/paralysis; and 5, moribund.

EAE induced animals were monitored daily up to 35 days postimmunization (dpi). End point evaluation included a variety of disease parameters which reflect the severity of the disease, such as the disease incidence and mortality, the day of disease onset, the mean maximum score, the mean score reached in the relapse and the chronic phases, and the cumulative score over the experimental time.

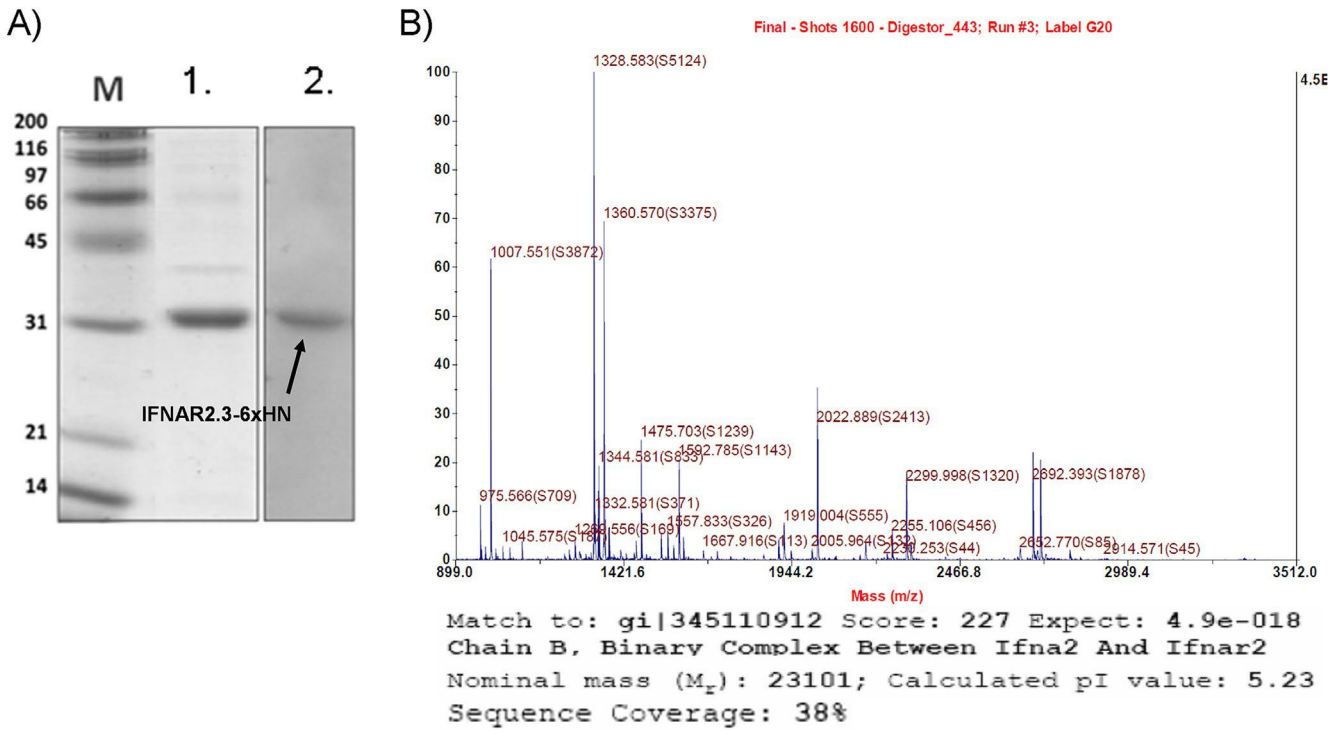

Fig. 1. A). Recombinant sIFNAR2 purified. M: molecular weight, 1.SDS-PAGE 12%; 2. Western Blot of purified sIFNAR2 (30 kDa). B) Protein identification by MALDI-TOF MS and peptide mass fingerprinting.

2.6. Treatment protocols

CP-EAE-induced animals were randomly distributed in groups of 12 mice to receive one of the following chronic treatments:

1) IFNb: 10.000 Units (40 ng) of recombinant murine IFNb (Mouse Interferon Beta, mammalian, carrier-free, PBL Interferon source).
2) IFNb þ sIFNAR2 as a combined therapy (IFNb/sIFNAR2): 40 ng each.
3) sIFNAR2: 40 ng.

To evaluate the clinical efficacy, drugs were administered once after the onset of disease, when the clinical score reached values between 0.5 and 1 (at 14 days post-immunization, dpi), and every 3 days up to the end of the experiment (35 dpi). Drugs were injected ip. For each injection, compounds were diluted in 200 ml saline as vehicle. EAE-control mice group (n ¼ 6) received only vehicle (200 ml saline) by similar protocols.

2.7. Tissue extraction and processing

EAE-induced animals were sacrificed by intraperitoneal administration of a lethal dose of pentobarbital. Fresh extraction of spleen, brain and spinal cord were performed at the chronic period (35 dpi). Spleens were placed in Hibernate® medium (Life Technologies) until their processing to the lymphocyte subpopulations study. The lumbar spinal cord zones were placed in 4% PFA (Sigma-Aldrich Química S.L.), cryoprotected in 30% (w/v) sucrose, and cut in 40 m cryostat sections for their histopathological analysis.

2.8. Flow cytometry analysis of splenic subsets

After removing the Hibernate® medium, a single splenocyte suspension was obtained from spleens by passing them through a 40 m nylon cell strainer (BD Falcon). After red blood cell lysis in ACK lysis buffer (8.29 gr/L NH_4Cl, 1 gr/L CO_3HK, 1 mM EDTA in distilled H_2O pH 7.4: Panreac), 10^6 splenocytes were resuspended in 50 ml of staining buffer (sterile PBS supplemented with 25 mM HEPES, 2% Penicillin/Streptavidin, and 10% Foetal Bovine Serum (FBS, Linus) and the Fc receptors were blocked for 10 min at 4 °C with anti-CD16/CD32 antibodies (10 mg/ml; BD Biosciences). After blocking, the cells were labeled for an additional 30 min at 4 ° C in the dark with 50 ml of the corresponding antibody panel in staining buffer. Splenocytes were washed twice with staining buffer, they were recovered by centrifugation at 1500 rpm for 5 min at RT, resuspended in PBS and finally, the samples were assayed in a FACS Canto II cytometer (BD Biosciences). Antibodies from the lymphoid panel included a FITC-conjugated anti-mouse CD8, R-PE-conjugated anti-mouse CD4, Pacific Blue-conjugated anti-mouse CD3þ (from BD Biosciences), APC-conjugated anti-mouse CD69 (from eBiosciences) and isotype controls conjugated with FITC, R-PE, Pacific Blue, and APC. The data were analyzed by gating on CD3þ cells with FlowJo 7.6.4 software (TreeStar Inc.).

2.9. Immunohistochemistry analysis of histopathology in CNS

Immunohistochemistry was carried out by IBIMA (Ma laga, Spain) common research facilities (ECAI) of Image, by the following protocols: analysis of spinal T-cell infiltrates and demyelination were performed by free-floating immunostaining of 40 m slices using antibodies against the CD3 antigen (rabbit polyclonal, 1:100) combined with conventional Luxol Fast Blue staining (LFB). Microglial activation and oligodendrocyte population, were determined by free-floating immunostaining using antibodies against Iba 1 (goat polyclonal, 1:1000) and oligodendrocyte transcription factor (Olig2, rabbit polyclonal, 1:750), respectively. Neuronal populations were evaluated by using NeuN (mouse monoclonal, 1:500; Millipore, Billerica, MA) and MAP-2 (mouse monoclonal,

1:1000; Sigma-Aldrich Química, S.L.) antibodies. For their detection, Extravidin® peroxidase (Sigma-Aldrich Química, S.L.) and 3,3⁰-diaminobenzidine (Sigma-Aldrich Química, S.L.) methods were used as described previously (Marin-Barrasco et al., 2014).

Analysis were carried out over 4 x , 10 x and 20 x images (three or four images per animal/antibody) using a trinocular inverted phase contrast microscope (Leica DMIL LED; Leica Microsystems, Inc., Barcelona, Spain). Inflammatory infiltrates, microglial activation, Olig2, NeuN and MAP-2 positive cells were determined by counting the number of labeled cells in 200 mm. The area of demyelination, in which staining was negative for LFB, was expressed as the percentage of total myelinated area per section. Data are shown as the mean ± SEM of values obtained from 3e4 slices of 5e6 animals per experimental group. For the neuronal stainings, control groups from healthy mice were included.

2.10. Proliferative assays with CFSE

Splenocytes cells were isolated from C57 female mice by mechanical dissociation pressed through a 100 m nylon cell strainer (Becton Dickinson, Franklin Lakes, NJ, USA). Subsequently, red blood cells were removed using Lysing buffer (Sigma-Aldrich Química S.L., Madrid, Spain) and, from the resulting pellet, 20 x 10^6 cells were resuspended in 1 ml RPMI-1640 complete medium, 10% FBS (Gibco® by Life Technologies). An equal volume of PBS containing 2.5 mM carboxyfluorescein diacetate succinimidyl ester (CFSE) was added, and cells were incubated at room temperature for 12 min.

After washing, 5 x 10^4 cells were dispensed into 96-well plates and stimulated in duplicate (37 °C, 72 h) in the following conditions:

1 Positive control: medium containing 5 mg/ml concanavalin A (ConA, Sigma-Aldrich)
2 ConA and 1000 U/ml murine IFNb
3 ConA and 30 mg/ml sIFNAR2.
4 ConA and 1000 U/ml murine IFNb þ30 mg/ml sIFNAR2
5 Non-dividing Control: Cells without stimulus

Cells were stained using rat monoclonal antibody (mAb) against mouse CD3 conjugate to peridinin chlorophyll protein-Vio 700 (PerCP-Vio 700), rat mAb against mouse CD4 conjugate to phycoerythrin-Vio 770 (PE-Vio 770) and rat mAb against mouse CD8a conjugate to allophycocyanin-Vio 770 (APC-Vio 770) (Miltenyi Biotec GmbH, Germany), as appropriate, for 10 min at 4 °C. Isotype-matched controls were used to verify the staining specificity of the antibodies. At least, 30.000 events were acquired in FACS Canto II flow cytometer (Becton Dickinson, USA) and analyzed with the FacsDiva software (Becton Dickinson, USA). Results were expressed as percentages of dividing cells. The experiment was performed three times.

2.11. Determination of pSTAT1 by flow cytometry

Cells isolated from two mouse spleens were seeded in RPMI-1640 medium without FBS and incubated at 37 °C for 90 min, in order to obtain the lowest level of activation. After that, cells were stimulated in duplicate in different conditions during 30 min to allow the signal transduction and the phosphorylation of the proteins:

1 IFNb (5000UI)
2 Different concentrations of sIFNAR2 (7.5, 15, 30, 60 and 90 mg/ml)
3 Different concentrations of sIFNAR2 (7.5, 15, 30, 60 and 90 mg/ml) with constant IFNb (5000UI)
4 Unstimulated cells

Following stimulation, the cells were fixed with Cytofix (BD Biosciences) at 37 ° C for 10 min, washed twice with Perm/Wash Buffer (BD Biosciences) and permeabilized with PermBuffer III (BD Biosciences) at 4 ºC for 20 min. After two additional washes, the cells were stained for 30 min with mAb against mouse and human phospho-STAT1 (Y701)-PE (Miltenyi Biotec GmbH, Germany), and CD3- PerCP-Vio 700 (Miltenyi Biotec GmbH, Germany),, as well as with the correspondent isotype-matched controls. Previously, the antibodies were titrated for optimal separation and staining. Cells were acquired and analyzed using the FACSDiva software, with at least 50,000 events per sample. Unstimulated cells were considered as basal levels. The data were analyzed as percentages of positive cells expressing pSTAT1.

2.12. MxA expression by real time PCR

From each mouse spleen, 1.10^6 T cells per ml were seeded in the following conditions, in duplicate, during 8 h without stimulation and stimulated with:

1 IFNb (5000UI)
2 Different concentrations of sIFNAR2 (7.5,15, 30, 60 and 90 mg/ml)
3 Different concentrations of sIFNAR2 (7.5, 15, 30, 60 and 90 mg/ml) with constant IFNb (5000UI)

To determine the MxA expression cells were collected by centrifugation and resuspended in QIAzol Lysis Reagent for RNA extraction. Total RNA was isolated from cells using a modification of the phenolechloroform method (Chomczynski and Sacchi, 1987). Total RNA yield and quality of product was assessed with a Nanodrop 2000 Spectrophotometer. For complementary DNA (cDNA) synthesis, 1 mg of total RNA was reverse transcribed with the M-MLV reverse transcriptase as described elsewhere (Oliver et al., 2007). Quantitative PCR was performed in duplicate in a Rotor Gene Q Thermocycler (Qiagen GmbH) using RT² qPCR Primer Assay (Quiagen), KAPA SYBR® FAST Universal One-Step qRT-PCR (Kapa Biosystems) and cDNA. The programme consisted of a step of 20 s at 95 °C, followed by 45 cycles of 95 °C for 3 s, 60 °C for 25 s. A melting step from 75 ° C to 95 ° C was run, increasing 0.5 °C every 5 s. The relative expression of MxA was calculated according to the 2−DDCT method (Livak and Schmittgen, 2001), by normalising to GAPDH expression.

2.13. Statistical analysis

The data were expressed as the mean ± SEM and were analyzed with SigmaStat (SPSS Inc., IBM Corporation, New York, USA). Student's *t*-test was performed to compare the mean values of clinical features of end point between different groups. To flow cytometry analysis, Kruskal-Wallis one way ANOVA on Ranks test was used for comparative analyses between the different groups followed by a multiple comparison procedure (Dunn's method) to isolate the group that differs from the other. Statistical differences between groups of immunohistochemistry parameters were determined by using one way ANOVA followed by *Newman-Keuls post hoc.* Minimal statistical significance was set at $P < 0.05$.

3. Results

3.1. Clinical effects of sIFNAR2 in CP-EAE

The CP-EAE model used in this study is characterized by a chronicеprogressive type of neurological deficit. The clinical course was marked by the appearance of a relapse, followed by a moderate period of symptomatic remission, which continued with a period of chronicity of symptoms (Fig. 2). Incidence of CP-EAE was 98%, with no significant differences on the day of the disease onset between the experimental groups (10.8 ± 0.2 dpi) (Table 1). Control mice, treated chronically with saline from 11 dpi until the end of the experimental period, suffered increased neurological deficit over time (relapse phase, from 9 to 19 dpi), and later presented a stable clinical course (chronic phase, from 20 to 35 dpi), typical of this chronic model (Fig. 2), as we published before (Marin-Banasco et al., 2014; Moline,-Vela,zquez et al., 2011, 2014). They showed an aggressive disease progression, as reflected by the highest maximum and cumulative mean scores (Table 1).

As expected, mice treated with INFb showed a decrease in the severity of the clinical course, represented in the reduction of the mean maximum score (2.4 ± 0.3 vs. 2.8 ± 0.1) and in the cumulative score reached (50.4 ± 5.5 vs. 59.6 ± 1.8) when compared with control animals (Fig. 2). Moreover, this treatment reduced the severity of both, the relapse and the chronic phases, even reaching statistically significant differences in the latter (1.9 ± 0.3 vs. 2.4 ± 0.1) (Table 1).

Interestingly, when administered as a combined therapy (IFNb/sIFNAR2), sIFNAR2 was able to potentiate the efficacy of IFNb. Animals suffered a very moderate EAE clinical course (Fig. 2) and showed a significant reduction in all the evaluated parameters related to the severity of the disease, reaching the lowest value of cumulative scores registered from all experimental groups (40.1 ± 2.9) (Table 1).

Surprisingly, the chronic treatment with sIFNAR2, administered as a monotherapy, induced *per se* a pronounced decrease of neurological deficit over the entire EAE clinical course, which was evident even from the first administered dose (Fig. 2). We found

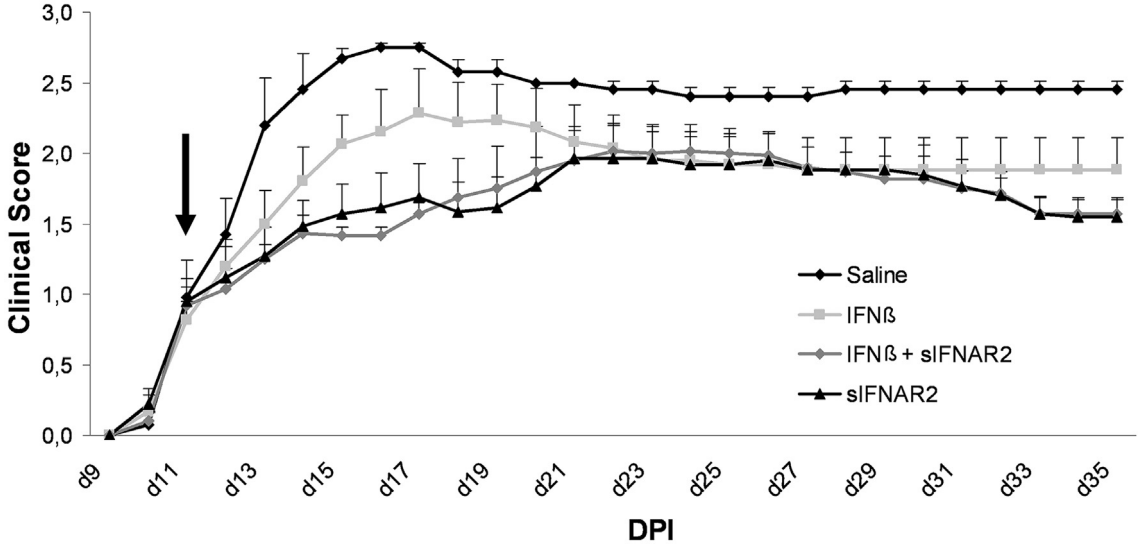

Fig. 2. Clinical outcome of chronic progressive experimental autoinmune encephalomyelitis (CP-EAE) mice treated with saline, IFNb, sIFNAR2 or combined therapy (IFNb þ sIFNAR2). The values are presented as mean ± standard error of the mean (SEM). Graph shows the clinical score progression of EAE model over the experimental period (up to 35 DPI, post-immunization days). Black arrow points to the day at which the treatment started. Treatments were administered from this day and each three days until the end of the experimental time. N ¼ 11e12 animals per experimental group.

Table 1
Clinical features of end point evaluation from CP-EAE mice treated with saline, IFNb, the combined therapy of IFNb þ sIFNAR2 or sIFNAR2.

Experimental group: CP-EAE	Disease incidence	Mortality	Day disease onset[a]	Mean maximum score[b]	Mean cumulative score[c]
SALINE	11/12	0/11	10.8 ± 0.3	2.8 ± 0.1	59.6 ± 1.8
IFNb	12/12	0/12	10.7 ± 0.2	2.4 ± 0.3	50.4 ± 5.5
IFNb þ sIFNAR2	12/12	0/12	10.8 ± 0.2	2.3 ± 0.2*	40.1 ± 2.9***
sIFNAR2	12/12	0/12	10.5 ± 0.2	2.2 ± 0.2*	44.2 ± 3.9**

	Mean score of relapse phase (9e19 dpi)[d]	Mean score of chronic phase (20e35 dpi)[d]
SALINE	1.9 ± 0.3	2.4 ± 0.1
IFNb	1.5 ± 0.3	1.9 ± 0.3**
IFNb þ sIFNAR2	1.1 ± 0.2	1.8 ± 0.2**
sIFNAR2	1.2 ± 0.2	1.8 ± 0.1**

Values are presented as mean ± standard error of the mean. Statistical analysis to perform single comparisons was carried out using Student's *t*-test. *P < 0.05, **P < 0.01, ***P < 0.0001 vs. saline.

[a] Day disease onset is defined as the first day in which animals showed any clinical symptoms (clinical score 2:0.5).

[b] Mean maximum score was the average of the maximum punctuation reached in the clinical scale by each animal in each experimental group.

[c] Mean cumulative score was average of accumulated EAE scores from each mouse over the entire experiment (until 35 dpi, days post-immunization).

[d] Mean score of each phase was the average of EAE scores from each experimental group over the relapse (from 9 to 19 dpi) or chronic (from 20 to 35 dpi) phases, respectively.

statistically significant differences in the reduction not only of the mean maximum (2.2 ± 0.2 vs. 2.8 ± 0.1) and cumulative scores (44.2 ± 3.9 vs. 59.6 ± 1.8) but also in the mean score of chronic phase, when compared with saline treated animals (Table 1). This effect was even stronger than that produced by the monotherapy with IFNb, presenting lower absolute values in all parameters evaluated (Table 1). Moreover, in these experiments, the clinical efficacy of the soluble protein was comparable to that induced by the combined treatment.

3.2. Peripheral effects of sIFNAR2: splenic subsets analysis

In order to know whether the clinical score amelioration has a parallel with peripheral T lymphocyte activation, the spleens of the four different groups of treated mice were analyzed. There were no differences in the percentage of T cells in the spleen of the different animal groups, either in the whole CD3þ T cell population or in the CD4þ and CD8þ T cell subsets (Fig. 3AeC). The percentage of fully activated CD69þ T cells with respect to each T cell subset (CD3, CD4, CD8) did not show differences between the experimental groups (Fig. 3DeF). In contrast, the CD69 mean fluorescence intensity (MFI) in the T cell subpopulations showed that the CD4þ CD69þ T cells from the groups receiving slFNAR2 displayed a significant decrease in the CD69 MFI with respect to those receiving saline or IFNb alone (Fig. 3, G-I). On the other hand, the whole CD3þ CD69þ T cells did not present differences in their CD69 MFI between treatments, similar to that found in the CD8þ CD69þ T cell subset.

3.3. Effects of sIFNAR2 on cells proliferation

The antiproliferative effect of sIFNAR2 was evaluated on splenic T cells. As expected, the percentage of proliferating CD3þ T cells

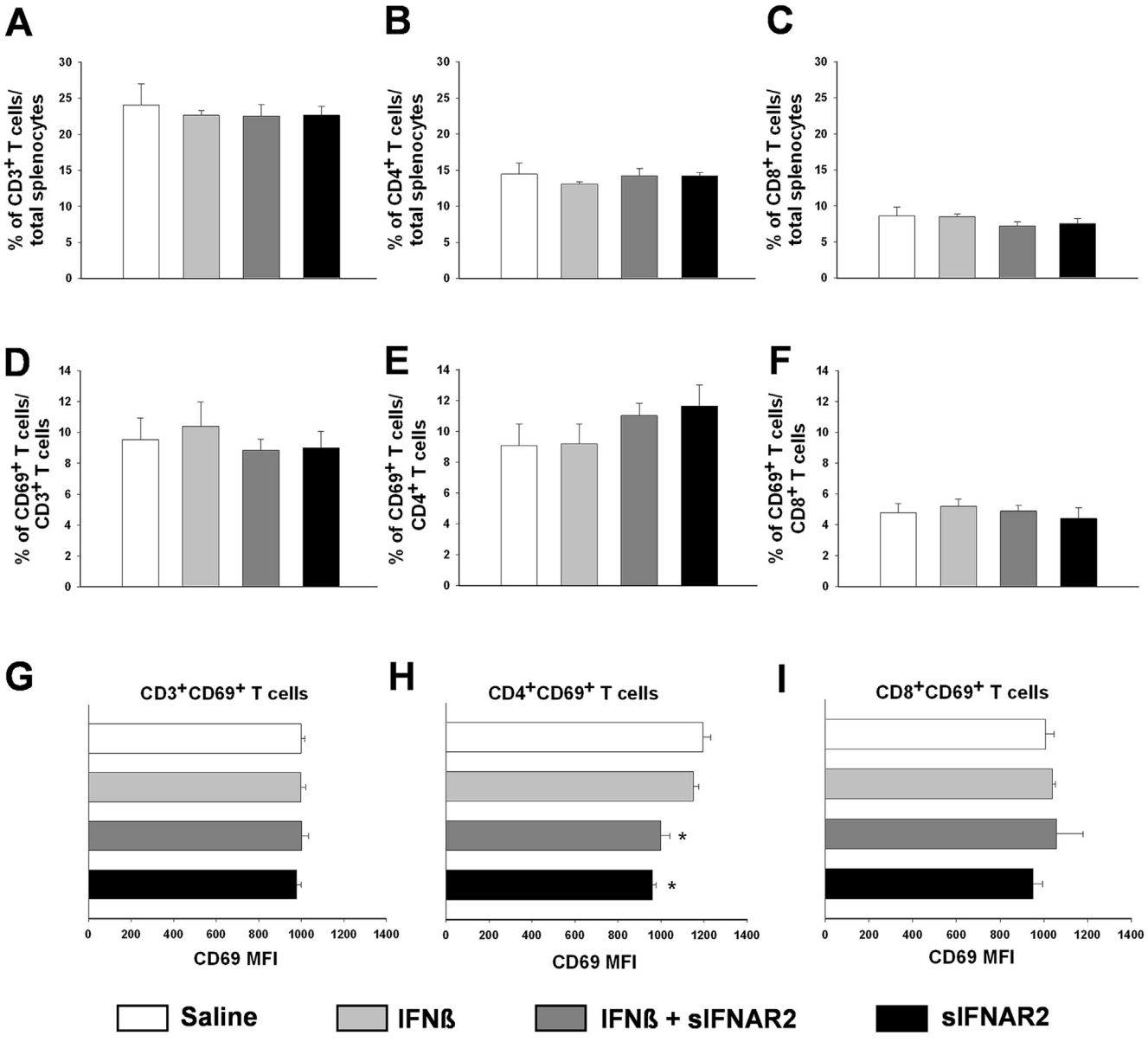

Fig. 3. Flow cytometry analysis of the T cell content within the spleen of the different treated groups at 35 DPI. AeC: Percentage of T cells in the spleen of the different animal groups: CD3 T cell population (A), CD4 (B) and CD8 T cell subsets (C). DeF: Percentage of fully activated CD69þ T cells with respect to each T cell subset (CD3, D; CD4, E; CD8, F). GeI: Plots of the CD69 mean fluorescence intensity (MFI) in the subpopulations described in D-F. For the statistical analysis, Kruskal-Wallis one way ANOVA on Ranks was carried out of the four groups followed by the *post hoc* Dunn's Method when appropriate. *P < 0.05.

after stimulation with ConA (32.5 ± 19.6), was decreased with the addition of murine IFNb (21.2 ± 13.2). The presence of sIFNAR2 potentiated the IFNb effect by decreasing the proliferation respect to IFNb alone (1.8 ± 0.7). Moreover, sIFNAR2 showed an important antiproliferative capacity *per se*, diminishing significantly the percentage of proliferating CD3þ T cells (3.2 ± 1.9), compared to ConA positive control and to IFNb alone (Fig.4, A). Similarly, sIFNAR2 showed a strong antiproliferative activity on CD4þ (Fig.4, B) and CD8þ T cells (data not shown).

3.4. Central effects of sIFNAR2: spinal cord analysis

Finally, we processed the spinal cords of each experimental group, at the end of the chronic phase (35 dpi), in order to evaluate whether there was a correlation between the observed clinical score amelioration and a reduction of the neurohistopathological damage in CNS. As expected, immunohistochemistry staining of spinal cord sections from chronified EAE saline-treated mice showed an important presence of T cell infiltrates (10.1 ± 0.9) accompanied by a considerable percentage of demyelination (19.9 ± 1.7), assessed by anti-CD3 antibody staining combined with LFB conventional staining, respectively (Fig.5). The IFNb treatment induced a reduction in the number of the CD3-positive cells although it did not reach statistical signification (8 ± 2) when compared to control animals (Fig.5A). On the other hand, the total demyelinated area, represented by the absence of LFB staining, was clearly diminished by the immunomodulator, reaching significant differences (11 ± 4.1) in comparison to control animals (Fig.5B). When this cytokine was administered in combination with sIFNAR2, the infiltrates (4.0 ± 1.2) and the percentage of the total demyelinated area (5.0 ± 1.4) were significantly reduced when compared with the control group. These values were also lower than those obtained after IFNb monotherapy, suggesting that the presence of sIFNAR2 potentiates the effect of IFNb.

Surprisingly but consistent with the clinical data, the effect of the monotherapy with sIFNAR2 was very noticeable, not only by reducing the T-cell infiltrates (1.4 ± 0.4 vs. 10.1 ± 0.9) (Fig.5A) but also the percentage of the total demyelinated area in the white matter of the lumbar spinal cord (1.8 ± 0.6 vs. 19.9 ± 1.7) (Fig. 5B) when compared with animals treated with saline. It is worthy to

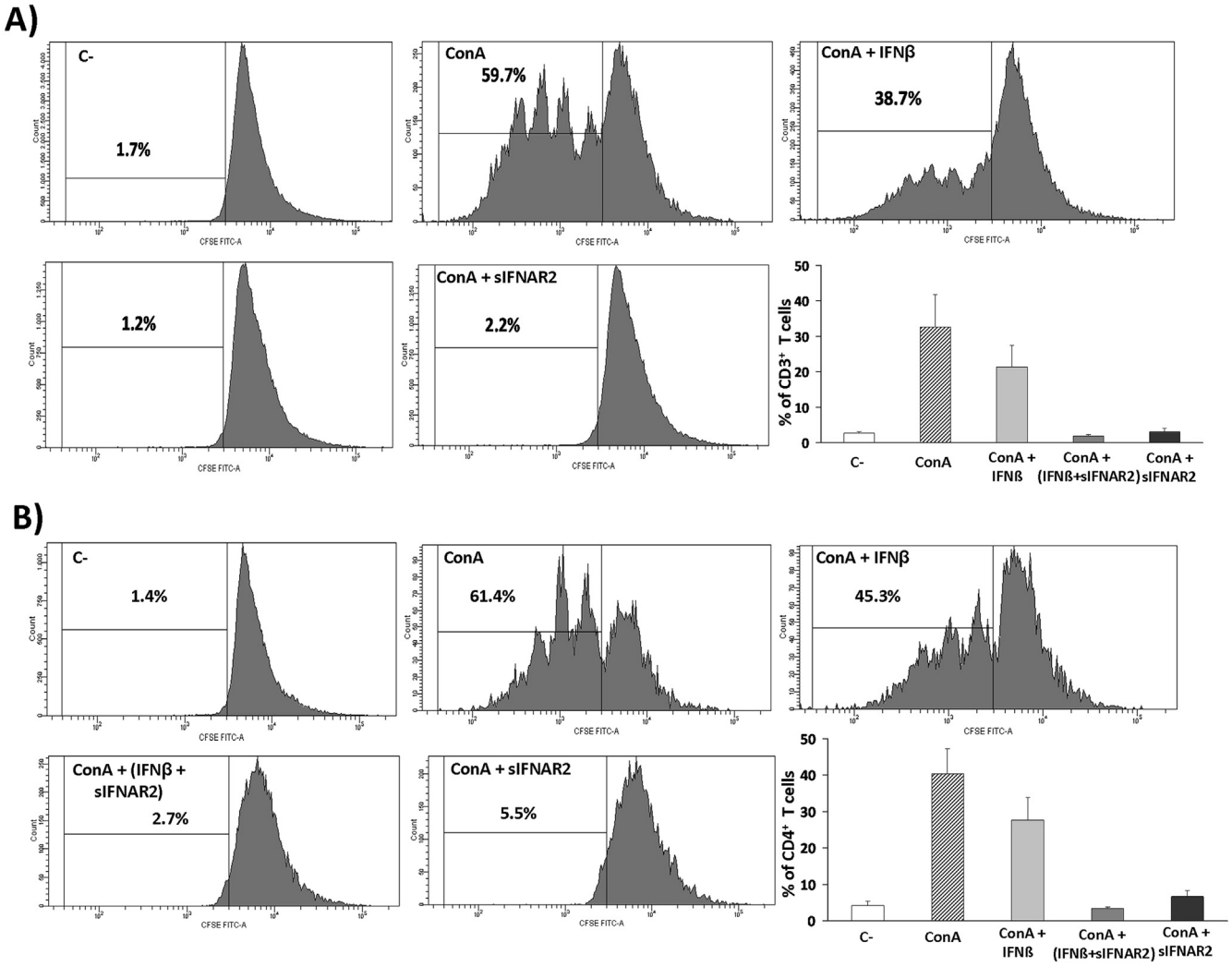

Fig. 4. Effects of sIFNAR2 on cells proliferation. Spleen T cells were incubated with CFSE to asses the proliferation in the following conditions: Without stimulus (C-); concanavalin A (ConA, 5 mg/ml); ConA þ IFNb (1000 U/ml); ConA þ [IFNb (1000 U/ml) þ sIFNAR (30 mg/ml)]; ConA þ sIFNAR2 (30 mg/ml). Following 72 h of incubation, the cells were stained with monoclonal antibody against mouse CD3 conjugate to PerCP-Vio 700 (A) and monoclonal antibody against mouse CD4 conjugate to phycoerythrin-Vio 770 (PE-Vio 770) (B). CFSE cell proliferation data were acquired in FACS Canto II flow cytometer and analyzed with the FacsDiva software. Representative histograms of each condition are shown. Data are expressed as means ± SE (3 independent experiments in duplicate, per condition) and represented as bar diagram.

distinguish that sIFNAR2 induced the most pronounced decrease of these two parameters (T cell infiltration and demyelination) in comparison to the rest of the experimental therapies, reaching significant differences when compared to control and IFNb-treated animals.

The microglial activation was considered as an indicator of the inflammatory state so, in order to test it, the lumbar spinal cord sections were stained with anti-Iba1, which allows the discrimination of the activated microglial cells. The number of activated microglial cells located in the spinal cords of IFNb-treated animals was clearly diminished when compared to saline-treated animals (1.6 ± 0.3 vs. 3.3 ± 0.4) (Fig.6). When both the immunomodulator and the soluble molecule were administered together, the treatment induced a higher reduction in the number of activated microglia (1.3 ± 0.4 vs. 3.3 ± 0.4) when compared to controls. Interestingly, the decrease in activated microglial cells in animals which only received sIFNAR2 was of the same extent (1.2 ± 0.2 vs. 3.3 ± 0.4).

We also tested the efficacy of the experimental therapies on the survival of neuronal population by counting the number of NeuN and MAP-2 positive cells in the spinal cord grey area. Results showed that no statistically significant differences were found in the dorsal horn of NeuNþ and MAP-2þ neuronal populations among mice, irrespective of the received treatment nor comparing to healthy controls (Data not shown). However, there was a significant increment in the number of the NeuN þ neurons of the ventral horns induced by sIFNAR2 (16.1 ± 1) in comparison to non-EAE induced (healthy) animals (12.7 ± 1.5), to animals receiving saline (12.2 ± 0.6) or the combined therapy (12.7 ± 0.6) (Fig. 7A). Although we found a higher number of MAP-2þ neurons in the ventral horns from animals receiving sIFNAR2 (27.8 ± 2.6) when compared to healthy control (24.5 ± 3,2) and animals treated with saline (21 ± 2), these differences did not reach statistical significance (Fig. 7B).

Finally, we analyzed the effects of therapies on oligodendrocyte populations by using the antibody against the transcriptional factor Olig2, which is mainly expressed in these cells and, in case of tissue injury, is overexpressed in oligodendrocyte precursors favouring

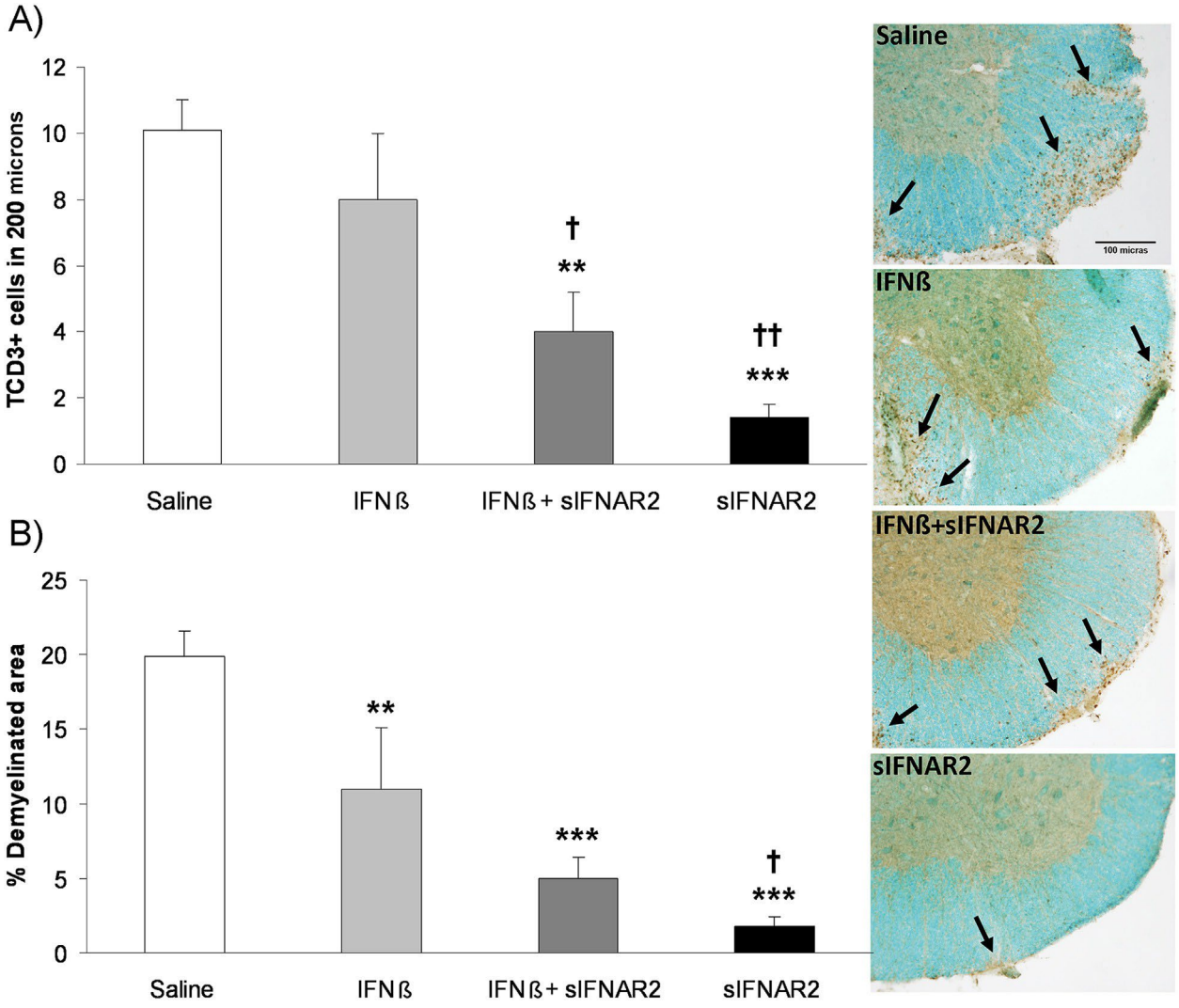

Fig. 5. Effects of treatments on inflammatory infiltrates A) and demyelination B) in the spinal cord of CP-EAE mice. Images represent lumbar spinal cord sections from EAE mice stained with anti-CD3 and counterstained with Luxol Fast Blue (LFB) to detect inflammatory T cells infiltrates and the degree of demyelination, respectively, which have been pointed to with black arrows. Magnification: 10x. Graphs show the mean ± standard error of the mean of the number of A) T cells stained with CD3 in 200 mm and B) the percentage of demyelinated area, characterized by a lack of LFB staining, related to the total area. Analysis were performed from 3e4 sections of 5e6 animals per experimental group. Statistical analysis was carried out using one way ANOVA followed by *Newman-Keuls post hoc*. **P < 0.01; ***P < 0.001 vs. Saline; yP < 0.05; yyP < 0.01 vs. IFNb.

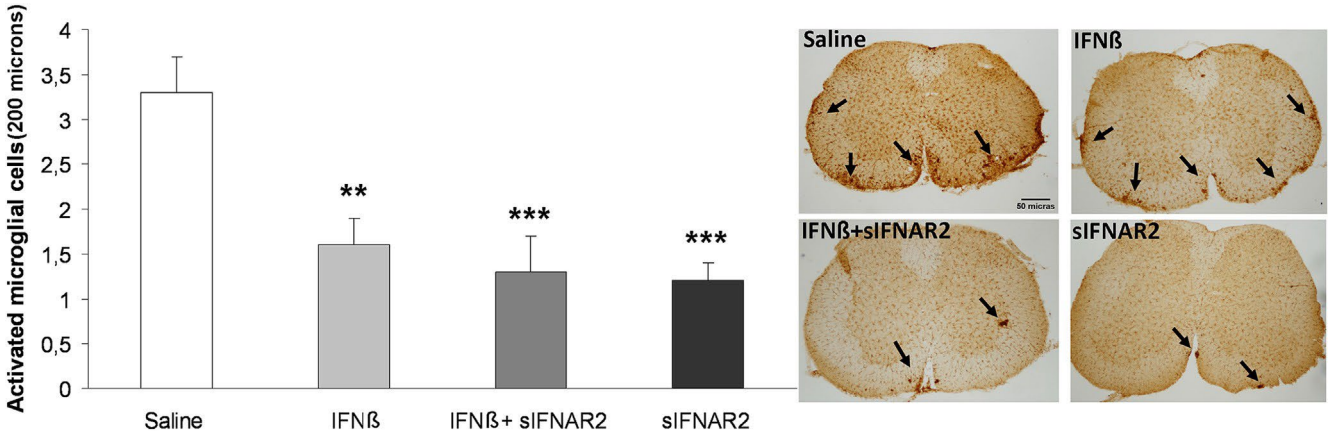

Fig. 6. Effects of treatments on activated microglia population in the spinal cord of CP-EAE mice. Images are representative from lumbar spinal cord sections from EAE mice stained with anti-iba1 to distinguish the activated microglial cells, which are pointed to with black arrows. Magnification: 4x. Graphs show the mean ± standard error of the mean of the number of activated microglial cells in 200 mm. Analysis were performed from 3e4 sections of 5e6 animals per experimental group. Statistical analysis was carried out using one way ANOVA followed by *Newman-Keuls post hoc*. **P < 0.01; ***P < 0.001 vs. Saline.

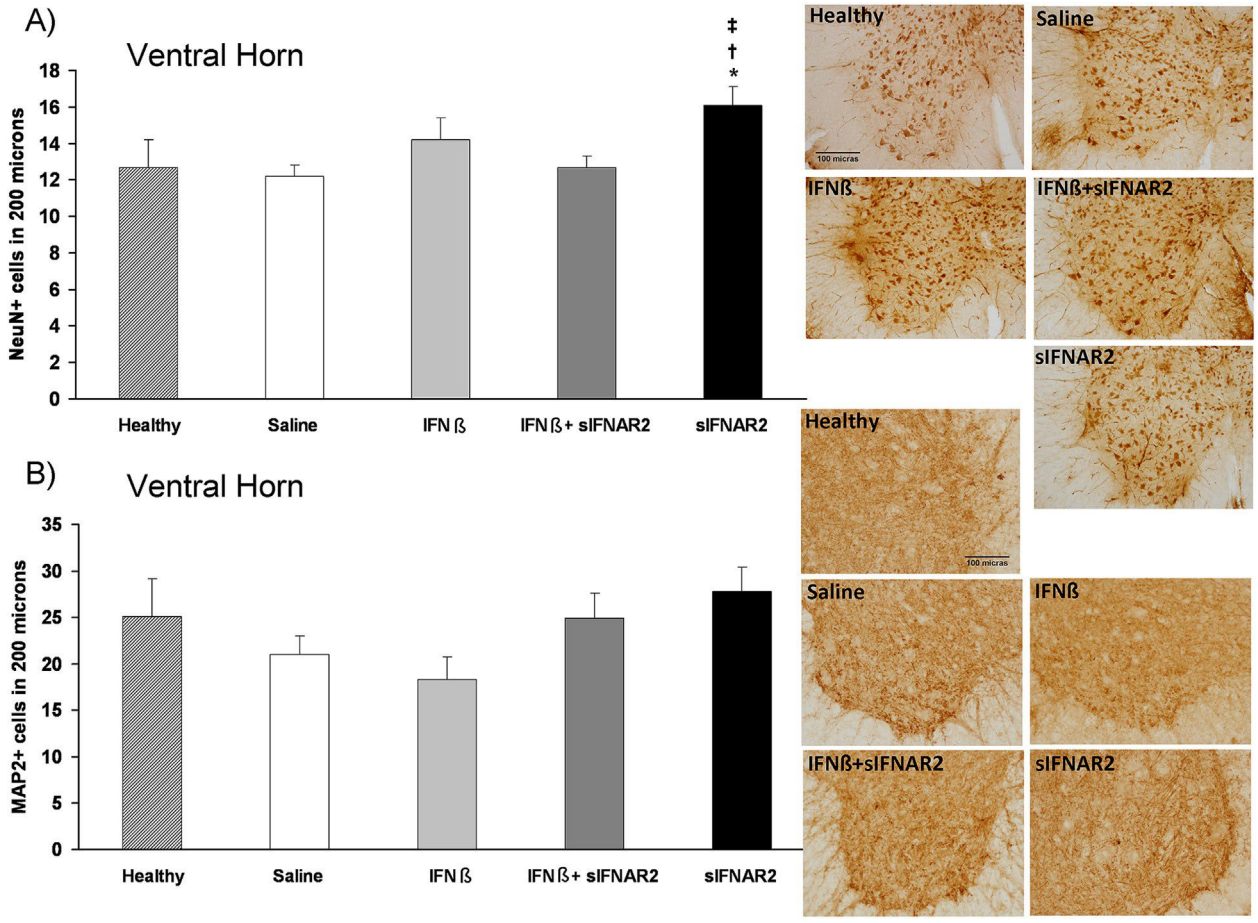

Fig. 7. Effects of treatments on neuronal population in the spinal cord of CP-EAE mice. Images are representative from lumbar spinal cord sections from EAE mice stained with A) anti-NeuN and B) anti-MAP-2, to label neurons. Control groups of healthy mice have been included. Magnification: 10x and 20x respectively. Graphs show the mean ± standard error of the mean of the number of A) NeuN and B) MAP-2 positive cells in 200 mm in ventral horn. Analysis were performed from 3e4 sections of 5e6 animals per experimental group. Statistical analysis was carried out using one way ANOVA followed by *Newman-Keuls post hoc*. *P < 0.05 vs. Healthy; γP < 0.05 vs. Saline; zP < 0.05 vs. IFNb þ sIFNAR2.

their differentiation to myelinating mature oligodendrocytes (Wegener et al., 2015). No differences were found in the spinal cords neither from animals treated with IFNb nor after its combination with sIFNAR2, when compared with control animals (Fig.8). However, a significant increment of the number of Olig2þ cells was evident after the treatment with sIFNARs (14.5 ± 1) compared with animals receiving any of the other therapies, i.e. saline (10.4 ± 0.6), IFNb (10.7 ± 0.9) and IFNb/sIFNAR2 (11.8 ± 0.8).

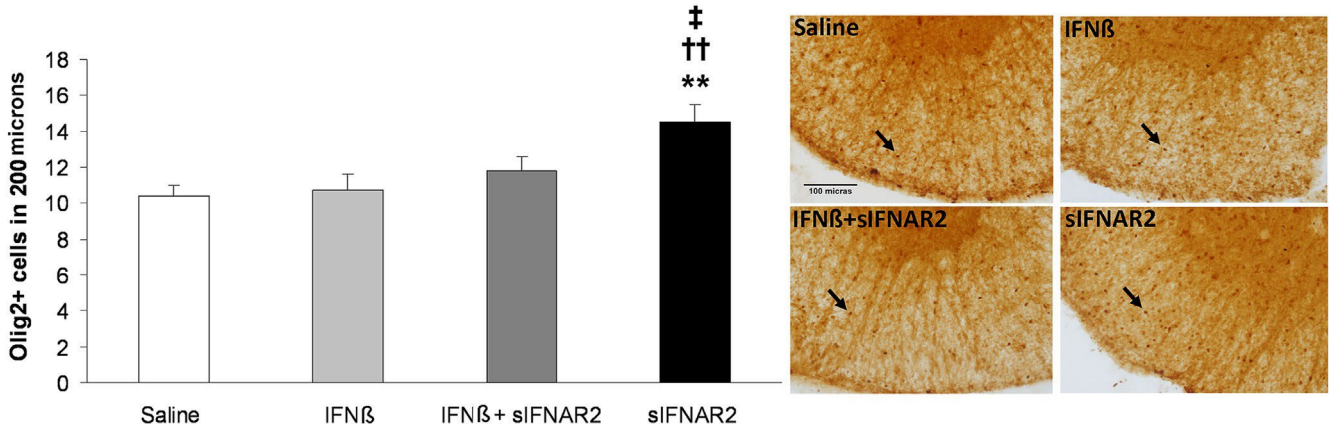

Fig. 8. Effects of treatments on oligodendrocyte populations in the spinal cord of CP-EAE mice. Images are representative from lumbar spinal cord sections from EAE mice stained with anti-Olig2 to label oligodendrocytes. Black arrows point to olig2 targets, which are represented by small brown spots. Magnification: 20 x . Graphs show the mean ± standard error of the mean of the number of Olig2 positive cells in 200. Analysis were performed from 3e4 sections of 5e6 animals per experimental group. Statistical analysis was carried out using one way ANOVA followed by *Newman-Keuls post hoc*. **P < 0.01 vs. Saline; yyP < 0.01 vs. IFNb; zP < 0.05 vs. IFNb þ sIFNAR2. (For interpretation of the references to colour in this figure legend, the reader is referred to the web version of this article.)

3.5. *Effects of sIFNAR2 on the IFNb signalling pathway (STAT1/MxA)*

In order to elucidate if sIFNAR2 could exert its effect through the IFNb signalling pathway, we evaluated in murine T cells the activation of STAT1 by flow cytometry and the mRNA expression of MxA, which is an IFNb-inducible protein and it is considered a biomarker of IFNb activity. As expected, after stimulation with IFNb, the percentage of pSTAT1 increased when compared to non-stimulated T cells (6.6 ± 0.6 vs. 0.8 ± 0.05). However, no significant activation of STAT1 was observed with any of the tested concentrations of sIFNAR2 (7.5e90 mg) as shown in Fig. 9A. Regarding the interaction with IFNb, increased concentrations of sIFNAR2 inhibited the activation of STAT1 induced by IFNb, in a dose dependent manner (Fig. 9B).

After stimulation with IFNb, the MxA mRNA was induced (95.6 ± 20.2). In the dose-response curve, sIFNAR2 failed to induce MxA, obtaining values similar to those observed without stimulation (Fig. 9C). In a similar way to what occurred with pSTAT1, the interaction sIFNAR2-IFNß showed that the highest doses of sIFNAR2 exerted an inhibition of the IFNb-induced MxA expression (Fig. 9D).

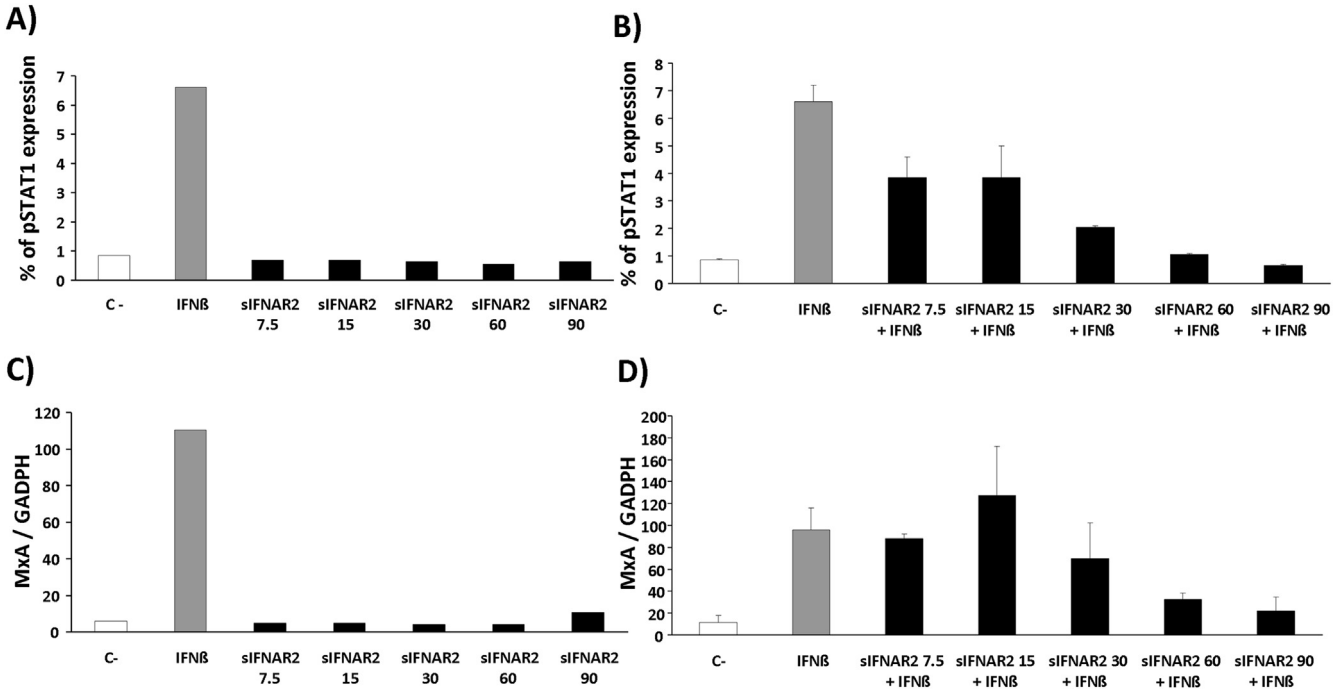

Fig. 9. Effects of sIFNAR2 on the IFNb signalling pathway (STAT1/MxA) in cells isolated from mouse spleens. pSTAT1 expression was determined in T cells after 30 min *in vitro* stimulation with: A) sIFNAR2, ranged from 7.5 mg to 90 mg. B) same concentrations of sIFNAR2 in presence of constant IFNb (5000 U). Relative MxA expression was determined in T cells after 8 h *in vitro* stimulation with: C) sIFNAR2, ranged from 7.5 mg to 90 mg. D) same concentrations of sIFNAR2 in presence of constant IFNb (5000 U). Two controls were included: a negative control (C-, without stimulation) and a positive control (IFNb, 5000UI). Graphs show the mean ± standard error of the pSTAT1 and the MxA expression obtained from duplicates in two independent experiments.

4. Discussion

Soluble receptors for cytokines normally participate in the control of cytokine activity and the ability of binding to the cytokine has prompted interest in their use as therapeutic agents. Concerning MS, the endogenous IFNb is one of the main cytokines that contributes to the maintenance of the anti-inflammatory status of the organism and it is involved in MS pathogenesis (Severa et al., 2015). Nevertheless, the role of its soluble receptor (sIFNAR2) as modulator of the IFNb activity in this disease has been poorly studied.

Previous experiments demonstrated that recombinant sIFNAR2 can bind IFN with nanomolar affinity (Arduini et al., 1999; Han et al., 2001; Hardy et al., 2001; Jaks et al., 2007; Piehler and Schreiber, 1999), and that is able to modulate type I IFN actions *in vitro,* as either an agonist or an antagonist, analogous to other soluble cytokine receptors (Hardy et al., 2001; McKenna et al., 2004; Samarajiwa et al., 2014). However, to our knowledge, there is no direct evidence for an *in vivo* function of this molecule by itself, so far. For all these reasons we have studied the effect of sIFNAR2 in the EAE model, that shares clinical and neuropathological changes with the MS human disease, and in which the potential efficacy of sIFNAR2 has not been previously evaluated. The human recombinant sIFNAR2, cloned in our laboratory, was administered as a combined therapy with IFNb (IFNb/sIFNAR2) or as monotherapy (sIFNAR2) into EAE-CP induced mice. With this approach, we expected to evaluate not only the possible interaction between the effects of both proteins but also the effects of sIFNAR2 *per se*.

First, the known clinical efficacy of IFNb in EAE models (Khorooshi et al., 2015; Kocur et al., 2015; Martin-Saavedra et al., 2007) was corroborated by our present results, since the IFNb ameliorated the EAE clinical course when compared to animals treated with saline. Although no peripheral effects were found after IFNb treatment on the percentage of the splenic T cell populations or on their activation state, there was a reduction of both central inflammation and demyelination, as reflected in a reduction in the activated microglia and the total demyelinated area.

After the combined therapy administration, the clinical course of the CP-EAE in mice was also modified. The clinical parameters evaluated showed that the addition of both, the cytokine and its soluble receptor, was effective in reducing the severity of the symptoms, being all values clearly lower than those obtained after IFNb monotherapy. These results suggest that the soluble protein could potentiate the clinical effects of IFNb. Although the present study is the first in evaluating the role of the combined cytokine treatment in EAE, our results are consistent with those from other authors that have tested the *in vivo* interaction between IFNb and its soluble receptor in other experimental models; The group of McKenna et al. (2004) has demonstrated that sIFNAR2 can bind to IFNb and then potentiate its effects in a dose-dependent manner in an experimental model of cancer. More recently, Samarajiwa et al. (2014) have suggested that sIFNAR2 is an important agonist of endogenous IFN effects, and also may modulate the therapeutic efficacy of clinically administered IFNs in a mouse model of septic shock, highlighting the importance of IFNb-sIFNAR2 axis in regulating the cytokine bioactivity.

Moreover, histopathological analysis confirmed that clinical amelioration induced by IFNb/sIFNAR2 was accompanied by changes in cell populations at the peripheral and central levels. In order to check T cell activation state, we analyzed the percentage and MFI of CD69, a commonly used T cell activity marker in EAE (Szalai et al., 2007; Tran et al., 2000) and MS (Arneth, 2015; Jensen et al., 2006). Although no effects were found over the total number of splenic T lymphocytes, there was a down-regulation of CD69 on CD4þ T lymphocytes with no signs of any alteration on the CD8þ cell subset. The reduction of CD69 on CD4þ T cells has been previously considered a sign of EAE amelioration after therapeutic treatments affecting the EAE clinical course (Fang et al., 2014).

In the spinal cord, the size of the demyelinated and cell infiltration areas and the microglia activation were significantly reduced after the combined treatment, showing again the potentiation of the immunomodulatory effects of IFNb. Although no previous works have evaluated in the EAE model the inmmunodulatory effects of IFNb in presence of recombinant sIFNAR2, it has been postulated that IFNb could bind to its soluble receptor, which could increase its half-life and its bioavailability and, therefore, enhance their therapeutic effects (Samarajiwa et al., 2014). In addition, other reports demonstrate that soluble cytokine receptors can function as carrier proteins for their ligand and, subsequently, can protect it from proteolysis, improve its stability, modulate its tissue distribution, or decrease its clearance (Aderka et al., 1992; Ma et al., 1996).

On the other hand, the neuroprotective effects (protection of the neuronal populations and promoting the tissue repair mechanisms orchestrated by oligodendrocytes) did not reach statistical signification either with IFNb alone or accompanied by sIFNAR2. Although, some bibliography of the neuroprotective effects of IFNb exists (Khorooshi et al., 2015; Kocur et al., 2015) studies related to the effects of sIFNAR2 are lacking, so further experiments in order to elucidate its role in neuroprotection are warranted.

Surprisingly, the chronic administration of recombinant sIFNAR2 protein in monotherapy modified the EAE course compared to control animals, and induced: 1) an important reduction in the severity of the progression of EAE neurological deficits; 2) a reduction in the activation state of the splenic CD4þ T cell population; 3) an amelioration of both inflammation (T cell infiltrates and activated microglia) and demyelination within the CNS; 4) an increased number of NeuN þ neurons and oligodendroglial populations in the ventral zones of lumbar spinal cord. Altogether, these results indicate that sIFNAR2 could play an important role in counteracting the inflammatory processes occurring during the disease, as well as in neutralizing the characteristic neurodegenerative processes that occurred after the long-term progression of this CP-EAE model (Berard et al., 2010; Miller and Karpus, 2007).

Therapy with sIFNAR2 appeared even more effective than the IFNb therapy, by inducing a more pronounced amelioration of the severity of the EAE clinical course, the inflammation, the tissue damage and the neurodegeneration induced in CP-EAE animals. Furthermore, the sIFNAR2 monotherapy seemed also to be more effective than the IFNb/sIFNAR2 therapy in ameliorating the evaluated neuroinflammatory processes and tissue damage. The interaction between the cytokine and its soluble receptor could enhance the IFNb clinical efficacy, as mentioned before, but it could also be hindering the effects of the sIFNAR2 at the same time, as sIFNAR2 could be exerting these intrinsic activity.

As sIFNAR2 was performing *per se* similar activities to IFNb, and taking into account the peripheral effects observed *in vivo* in splenic T cells, we evaluated the possible antiproliferative effect of sIFNAR2 *in vitro*. Similarly to other analyzed effects, sIFNAR2 was able to potentiate the known antiproliferative effect of IFNb, showing a functional interaction between them. Moreover, sIFNAR2 alone was also able to inhibit the proliferation of murine CD3þ T cells. Although a partial antiproliferative effect of murine sIFNAR2 in thymocytes has been previously reported (Hardy et al., 2001), to our knowledge, this is the first time that such a potent intrinsic effect of sIFNAR2, by dramatically inhibiting the ConA-induced T cell proliferation, has been described.

Finally, to evaluate if the action of recombinant sIFNAR2 is mediated by activation of classical IFNb signalling pathway (JAK-STAT), we determined, in murine spleen-T cells, two proteins

involved in this pathway, pSTAT1 and the biomarker of IFNb activity MxA (Bertolotto et al., 2015). The important activation of STAT1 and the induction of MxA expression after IFNb stimulation were not observed by sIFNAR2 for any of the concentrations tested, indicating that our recombinant sIFNAR2 is not able to activate *per se* the JAK-STAT signalling pathway. These results are in accordance with other experiments performed in our laboratory with different established cell lines and human cells, in which the activation of this pathway did not occur after sIFNAR2 stimulation (unpublished data). The alternative routes by which sIFNAR2 is exerting its activities need to be further investigated.

Otherwise, when cells were stimulated with constant IFNb and increasing sIFNAR2 concentrations, both pSTAT1 and MxA expression were modified. While lower concentrations of our recombinant sIFNAR2 slightly modify the expression of pSTAT1 and MxA induced by IFNb, higher concentrations of sIFNAR2 decreased the expression of both proteins, suggesting that the highest concentrations tested are saturating concentrations which decrease the availability of IFNb *in vitro*.

In conclusion, our recombinant sIFNAR2 is able to potentiate the IFNb immunomodulatory effects *in vivo*. At the same time, we should highlight the important intrinsic effects of sIFNAR2 in ameliorating the EAE disease and as a T cell antiproliferative molecule. Although its mechanisms of action are not yet elucidated, it could have potential therapeutic benefits in inflammatory diseases such as MS and, therefore, further investigations are justified.

Conflict of interest

Θ Ferna ndez received honoraria as consultant to advisory boards, and as chairman or lecturer in meetings, and has participated in clinical trials and other research projects promoted by Almirall, Actelion, Allergan, Bayer-Schering, Biogen-Idec, Novartis, Merck-Serono, Roche and Teva. The authors have no other relevant affiliations or financial involvement with any organization or entity with a financial interest in or financial conflict with the subject matter or materials discussed in the manuscript apart from those disclosed.

Acknowledgments

We gratefully acknowledge Ana I. Go mez-Conde and Lourdes Sa nchez-Salido from IBIMA Image ECAI (Common Research Facilities) for their technical assistance in the immunohistological procedures, Iris Sa nchez-Raya for her technical assistance and Dr. Virginia Vila-del Sol for her help with flow cytometry analysis. T Θ rpez-Zafra and MJ. Pinto-Medel have been supported by grants from Red Tema tica de Investigacio n Cooperativa Red Espan ola de Esclerosis Múltiple REEM (RD07/0060 and RD12/0032). This work was supported by grants from Consejería de Igualdad, Salud y Políticas sociales (Junta de Andalucía) to B Oliver-Martos (PI-0267-2013) and by grant from the Instituto de Salud Carlos III co-founded by Fondo Europeo de Desarrollo Regional - FEDER to B. Oliver-Martos (PI13/00927).

References

Aderka, D., Engelmann, H., Maor, Y., Brakebusch, C., Wallach, D., 1992. Stabilization of the bioactivity of tumor necrosis factor by its soluble receptors. J. Exp. Med. 175, 323e329.

Arduini, R.M., Strauch, K.L., Runkel, L.A., Carlson, M.M., Hronowski, X., Foley, S.F., Young, C.N., Cheng, W., Hochman, P.S., Baker, D.P., 1999. Characterization of a soluble ternary complex formed between human interferon-beta-1a and its receptor chains. Protein Sci. 8, 1867e1877.

Arneth, B., 2015. Early activation of CD4þ and CD8þ T lymphocytes by myelin basic protein in subjects with MS. J. Transl. Med. 13, 341.

Berard, J.L., Wolak, K., Fournier, S., David, S., 2010. Characterization of relapsing-remitting and chronic forms of experimental autoimmune encephalomyelitis in C57BL/6 mice. Glia 58, 434e445.

Bertolotto, A., Granieri, L., Marnetto, F., Valentino, P., Sala, A., Capobianco, M., Malucchi, S., Di Sapio, A., Malentacchi, M., Matta, M., Caldano, M., 2015. Biological monitoring of IFN-ß therapy in multiple sclerosis. Cytokine Growth Factor Rev. 26, 241e248.

Chomczynski, P., Sacchi, N., 1987. Single-step method of RNA isolation by acid guanidinium thiocyanate-phenol-chloroform extraction. Anal. Biochem. 162, 156e159.

Denic, A., Johnson, A.J., Bieber, A.J., Warrington, A.E., Rodriguez, M., Pirko, I., 2011. The relevance of animal models in multiple sclerosis research. Pathophysiology 18, 21e29.

Domanski, P., Witte, M., Kellum, M., Rubinstein, M., Hackett, R., Pitha, P., Colamonici, O.R., 1995. Cloning and expression of a long form of the beta subunit of the interferon alpha beta receptor that is required for signaling. J. Biol. Chem. 270, 21606e21611.

Fang, J., Han, D., Hong, J., Zhang, H., Ying, Y., Tian, Y., Zhang, L., Lin, J., 2014. SVa-MSH, a novel a-melanocyte stimulating hormone analog, ameliorates autoimmune encephalomyelitis through inhibiting autoreactive CD4(þ) T cells activation. J. Neuroimmunol. 269, 9e19.

Fernandez-Botran, R., 1991. Soluble cytokine receptors: their role in immunoregulation. FASEB J. 5, 2567e2574.

Fernandez-Botran, R., 1999. Soluble cytokine receptors: basic immunology and clinical applications. Crit. Rev. Clin. Lab. Sci. 36, 165e224.

Fernandez-Botran, R., 2000. Soluble cytokine receptors: novel immunotherapeutic agents. Expert. Opin. Investig. Drugs 9, 497e514.

Fischer, R., Kontermann, R.E., Maier, O., 2015. Targeting sTNF/TNFR1 signaling as a New therapeutic strategy. Antibodies 4, 48e70.

Friese, M.A., Montalban, X., Willcox, N., Bell, J.I., Martin, R., Fugger, L., 2006. The value of animal models for drug development in multiple sclerosis. Brain 129, 1940e1952.

Garg, N., Smith, T.W., 2015. An update on immunopathogenesis, diagnosis, and treatment of multiple sclerosis. Brain Behav. 5, e00362.

Han, C.S., Chen, Y., Ezashi, T., Roberts, R.M., 2001. Antiviral activities of the soluble extracellular domains of type I interferon receptors. Proc. Natl. Acad. Sci. U. S. A. 98, 6138e6143.

Hardy, M.P., Owczarek, C.M., Trajanovska, S., Liu, X., Kola, I., Hertzog, P.J., 2001. The soluble murine type I interferon receptor Ifnar-2 is present in serum, is independently regulated, and has both agonistic and antagonistic properties. Blood 97, 473e482.

Jaks, E., Gavutis, M., Uze, G., Martal, J., Piehler, J., 2007. Differential receptor subunit affinities of type I interferons govern differential signal activation. J. Mol. Biol. 366, 525e539.

Jensen, J., Langkilde, A.R., Frederiksen, J.L., Sellebjerg, F., 2006. CD8(þ) T cell activation correlates with disease activity in clinically isolated syndromes and is regulated by interferon-beta treatment. J. Neuroimmunol. 179, 163e172.

Khorooshi, R., Mørch, M.T., Holm, T.H., Berg, C.T., Dieu, R.T., Dræby, D., Issazadeh-Navikas, S., Weiss, S., Lienenklaus, S., Owens, T., 2015. Induction of endogenous Type I interferon within the central nervous system plays a protective role in experimental autoimmune encephalomyelitis. Acta Neuropathol. 130, 107e118.

Kocur, M., Schneider, R., Pulm, A.K., Bauer, J., Kropp, S., Gliem, M., Ingwersen, J., Goebels, N., Alferink, J., Prozorovski, T., Aktas, O., Scheu, S., 2015. IFNß secreted by microglia mediates clearance of myelin debris in CNS autoimmunity. Acta Neuropathol. Commun. 3, 20.

Livak, K.J., Schmittgen, T.D., 2001. Analysis of relative gene expression data using real-time quantitative PCR and the 2(-Delta Delta C(T)) Method. Methods 25, 402e408.

Ma, Y., Hurst, H.E., Fernandez-Botran, R., 1996. Soluble cytokine receptors as carrier proteins: effects of soluble interleukin-4 receptors on the pharmacokinetics of murine interleukin-4. J. Pharmacol. Exp. Ther. 279, 340e350.

Malyala, P., Singh, M., 2008. Endotoxin limits in formulations for preclinical research. J. Pharm. Sci. 97, 2041e2044.

Marin-Ban asco, C., Suardk az Garck a, M., Hurtado Guerrero, I., Maldonado S inchez, R., Estivill-Torr ss, G., Leyva Fern indez, L., Fern indez Fern indez, O., 2014. Mesenchymal properties of SJL mice-stem cells and their efficacy as autologous therapy in a relapsing-remitting multiple sclerosis model. Stem Cell Res. Ther. 5, 134.

Martin-Saavedra, F.M., Flores, N., Dorado, B., Eguiluz, C., Bravo, B., Garcia-Merino, A., Ballester, S., 2007. Beta-interferon unbalances the peripheral T cell proinflammatory response in experimental autoimmune encephalomyelitis. Mol. Immunol. 44, 3597e3607.

McKenna, S.D., Vergilis, K., Arulanandam, A.R., Weiser, W.Y., Nabioullin, R., Tepper, M.A., 2004. Formation of human IFN-beta complex with the soluble type I interferon receptor IFNAR-2 leads to enhanced IFN stability, pharmacokinetics, and antitumor activity in xenografted SCID mice. J. Interferon Cytokine Res. 24, 119e129.

Miller, S., Karpus, W., 2007. Experimental autoimmune encephalomyelitis in the mouse. Curr. Protoc. Immunol. 15.1.1e15.1.18. Supplement 78.

Moline -Vela zquez, V., Cuervo, H., Vila-Del Sol, V., Ortega, M.C., Clemente, D., de Castro, F., 2011. Myeloid-derived suppressor cells limit the inflammation by promoting T lymphocyte apoptosis in the spinal cord of a murine model of multiple sclerosis. Brain Pathol. 21, 678e691.

Moline -Vela zquez, V., Vila-Del Sol, V., de Castro, F., Clemente, D., 2015. Myeloid cell distribution and activity in multiple sclerosis. Histol. Histopathol. 11699.

Moline -Vel izquez, V., Ortega, M.C., Vila del Sol, V., Melero-Jerez, C., de Castro, F.,

Clemente, D., 2014. The synthetic retinoid Am80 delays recovery in a model of multiple sclerosis by modulating myeloid-derived suppressor cell fate and viability. Neurobiol. Dis. 67, 149e164.
Moreno, B., Espejo, C., Mestre, L., Suardiaz, M., Clemente, D., de Castro, F., Fern ̧indez-Fern ̧indez, O ́., Montalban, X., Villoslada, P., Guaza, C., Spanish Network for MS, 2012. Guidelines on the appropriate use of animal models for developing therapies in multiple sclerosis. Rev. Neurol. 54, 114e124.
Novick, D., Cohen, B., Rubinstein, M., 1992. Soluble interferon-alpha receptor molecules are present in body fluids. FEBS Lett. 14, 445e448.
Novick, D., Cohen, B., Tal, N., Rubinstein, M., 1995. Soluble and membrane-anchored forms of the human IFN-alpha/beta receptor. J. Leukoc. Biol. 57, 712e718.
Oliver, B., Mayorga, C., Fernandez, V., Leyva, L., Leon, A., Luque, G., Lopez, J.C., Tamayo, J.A., Pinto-Medel, M.J., de Ramon, E., Blanco, E., Alonso, A., Fernandez, O., 2007. Interferon receptor expression in multiple sclerosis patients. J. Neuroimmunol. 183, 225e231.
Orpez-Zafra, T., Pavia, J., Pinto-Medel, M.J., Hurtado-Guerrero, I., Rodriguez-Bada, J.L., Mart in Montan ̧ez, E., Fernandez, O., Leyva, L., Oliver-Martos, B., 2015. Development and validation of an ELISA for quantification of soluble IFN-ß receptor: assessment in multiple sclerosis. Bioanalysis 7, 2869e2880.
Piehler, J., Schreiber, G., 1999. Biophysical analysis of the interaction of human ifnar2 expressed in E. coli with IFNalpha2. J. Mol. Biol. 289, 57e67.
Platanias, L.C., 2005. Mechanisms of type-I- and type-II-interferon-mediated signalling. Nat. Rev. Immunol. 5, 375e386.
Probert, L., 2015. TNF and its receptors in the CNS: the essential, the desirable and the deleterious effects. Neuroscience 27, 2e22.
Rose-John, S., Heinrich, P.C., 1994. Soluble receptors for cytokines and growth factors: generation and biological function. Biochem. J. 300 (Pt 2), 281e290.
Samarajiwa, S.A., Mangan, N.E., Hardy, M.P., Najdovska, M., Dubach, D., Braniff, S.J., Owczarek, C.M., Hertzog, P.J., 2014. Soluble IFN receptor potentiates in vivo type I IFN signaling and exacerbates TLR4-mediated septic shock. J. Immunol. 192, 4425e4435.
Severa, M., Rizzo, F., Giacomini, E., Salvetti, M., Coccia, E.M., 2015. IFN-ß and multiple sclerosis: cross-talking of immune cells and integration of immunoregulatory networks. Cytokine Growth Factor Rev. 26, 229e239.
Steinman, L., Zamvil, S.S., 2005. Virtues and pitfalls of EAE for the development of therapies for multiple sclerosis. Trends Immunol. 28 (11), 565e571.
Steinman, L., Zamvil, S.S., 2006. How to successfully apply animal studies in experimental allergic encephalomyelitis to research on multiple sclerosis. Ann. Neurol. 60, 12e21.
Szalai, A.J., Hu, X., Adams, J.E., Barnum, S.R., 2007. Complement in experimental autoimmune encephalomyelitis revisited: C3 is required for development of maximal disease. Mol. Immunol. 44, 3132e3136.
Tran, E.H., Prince, E.N., Owens, T., 2000. IFN-gamma shapes immune invasion of the central nervous system via regulation of chemokines. J. Immunol. 164, 2759e2768.
Wegener, A., Deboux, C., Bachelin, C., Frah, M., Kerninon, C., Seilhean, D., Weider, M., Wegner, M., Nait-Oumesmar, B., 2015. Gain of Olig2 function in oligodendrocyte progenitors promotes remyelination. Brain 138, 120e135.